[2] W. Yu and R. Mittra, "A conformal FDTD software package modeling antennas and microstrip circuit components," *IEEE Antennas Propagat. Mag.*, vol. 42, pp. 28–39, Oct. 2000.
[3] G. Mur, "Absorbing boundary conditions for the finite-difference approximation of the time-domain electromagnetic field equations," *IEEE Trans. Electromagn. Compat.*, vol. 23, pp. 377–382, 1981.
[4] S. D. Gedney, "An anisotropic perfectly matched layer-absorbing medium for the truncation of FDTD lattices," *IEEE Trans. Antennas Propagat.*, vol. 44, Dec. 1996.

An Efficient PSTD Algorithm for Cylindrical Coordinates

Qing Huo Liu and Jiang Qi He

***Abstract*—A pseudospectral time-domain (PSTD) algorithm is developed to overcome limitations in the conventional solution methods for Maxwell's equations in cylindrical coordinates. It is based on the fast Fourier transform (FFT) representation of spatial derivatives and a centered grid. The main contributions of this algorithm are to eliminate the singularity problem at the axis and to allow a larger time step. It uses a coarse grid close to the Nyquist sampling density provided that the geometrical modeling does not require fine cells. It reduces the required number of unknowns and the number of time steps in the finite-difference time-domain (FDTD) method and is efficient for large-scale problems.**

***Index Terms*—Finite-difference time-domain (FDTD), perfectly matched layers (PML), pseudospectral time-domain (PSTD), time domain analysis.**

I. Introduction

The finite-difference time-domain (FDTD) method has been enjoying its widespread applications in the simulations of transient electromagnetic wave propagation and scattering since it was first proposed by Yee in 1966 [1]. However, as the available computer memory and computational speed grow rapidly so that increasingly large problems are being solved, the phase dispersion error also increases. Hence, the required grid density (number of cells per wavelength) in the FDTD method also increases in order to maintain the same accuracy.

In cylindrical coordinates, the conventional FDTD method encounters yet two more difficulties: 1) the requirement for a very small Δt because of the high concentration of cells near the cylindrical (z) axis and 2) the singularity at the cylindrical axis. Although, various remedies have been proposed, the treatment is not straightforward and requires extra manipulations and computation time. In this work we propose a pseudospectral time-domain (PSTD) method with a perfectly matched layer (PML) absorber for three-dimensional (3-D) cylindrical and two-dimensional (2-D) polar coordinates to overcome these difficulties and to significantly increase the solution efficiency.

II. Formulation

In the conventional FDTD method [1] for Maxwell's equations in cylindrical coordinates, a staggered Yee grid is used [2]. The central differencing scheme for spatial and temporal derivatives has a second-order accuracy.

Recently, a pseudospectral time-domain (PSTD) algorithm was proposed for electromagnetic and acoustic waves in an attempt to increase the order of accuracy [3], [4]. In this work, we develop the PSTD algorithm for electromagnetic waves in cylindrical coordinates. We use the fast Fourier transform (FFT) to approximate the spatial derivatives and the cylindrical PML [5]–[7] to eliminate the wraparound effect. Here we use the PML formulation originally proposed by Teixeira and Chew [5], and later improved by He and Liu [7] for cylindrical coordinates.

In cylindrical ($\rho,\ \phi,\ z$) coordinates, we define the complex coordinates ($\tilde{\rho},\ \tilde{\phi},\ \tilde{z}$) in the frequency domain according to $d\tilde{\rho}/d\rho = (a_\rho + i\omega_\rho/\omega)$, $\tilde{\phi} = \phi$, and $d\tilde{z}/dz = (a_z + i\omega_z/\omega)$, where the real variables a_η and ω_η ($\eta = \rho,\ z$) are the scaling and attenuation factors in the PML. Then, we can derive the time-domain split Ampere's law for a conductive medium as [7]

$$a_\phi\epsilon\frac{\partial E_\rho^{(\phi)}}{\partial t} + (\omega_\phi\epsilon + a_\phi\sigma)E_\rho^{(\phi)} + \omega_\phi\sigma\int_{-\infty}^{t} E_\rho^{(\phi)}(\tau)\,d\tau = \frac{1}{\rho}\frac{\partial H_z}{\partial\phi} - J_\rho^{(\phi)} \tag{1}$$

$$a_z\epsilon\frac{\partial E_\rho^{(z)}}{\partial t} + (\omega_z\epsilon + a_z\sigma)E_\rho^{(z)} + \omega_z\sigma\int_{-\infty}^{t} E_\rho^{(z)}(\tau)\,d\tau = -\frac{\partial H_\phi}{\partial z} - J_\rho^{(z)} \tag{2}$$

$$a_\rho\epsilon\frac{\partial E_\phi^{(\rho)}}{\partial t} + (\omega_\rho\epsilon + a_\rho\sigma)E_\phi^{(\rho)} + \omega_\rho\sigma\int_{-\infty}^{t} E_\phi^{(\rho)}(\tau)\,d\tau = -\frac{\partial H_z}{\partial\rho} - J_\phi^{(\rho)} \tag{3}$$

$$a_z\epsilon\frac{\partial E_\phi^{(z)}}{\partial t} + (\omega_z\epsilon + a_z\sigma)E_\phi^{(z)} + \omega_z\sigma\int_{-\infty}^{t} E_\phi^{(z)}(\tau)\,d\tau = \frac{\partial H_\rho}{\partial z} - J_\phi^{(z)} \tag{4}$$

$$a_\rho\epsilon\frac{\partial E_z^{(\rho)}}{\partial t} + (\omega_\rho + a_\rho\sigma)E_z^{(\rho)} + \omega_\rho\sigma\int_{-\infty}^{t} E_z^{(\rho)}(\tau)\,d\tau = \frac{\partial H_\phi}{\partial\rho} - J_z^{(\rho)} \tag{5}$$

$$a_\phi\epsilon\frac{\partial E_z^{(\phi)}}{\partial t} + (\omega_\phi\epsilon + a_\phi\sigma)E_z^{(\phi)} + \omega_\phi\sigma\int_{-\infty}^{t} E_z^{(\phi)}(\tau)\,d\tau = \frac{1}{\rho}\left(H_\phi - \frac{\partial H_\rho}{\partial\phi}\right) - J_z^{(\phi)} \tag{6}$$

where

$$a_\phi = \frac{1}{\rho}\int_0^\rho a_\rho(\rho')\,d\rho' \qquad \omega_\phi = \frac{1}{\rho}\int_0^\rho \omega_\rho(\rho')\,d\rho'. \tag{7}$$

The other set of equations for updating $\mathbf{H}$ can be obtained by duality. In the above, the split field components are defined such that

$$\mathbf{E} = \sum_{\zeta=\rho,\ \phi,\ z}\hat{\zeta}\sum_{\eta\neq\zeta}E_\zeta^{(\eta)} \tag{8}$$

and similarly for other field and source components. This formulation has the advantage that it has the same number of unknown split field components as in Cartesian coordinates.

In the PSTD algorithm, the spatial derivatives are approximated by an FFT algorithm. For 3-D cylindrical coordinates, the treatment of z derivative $\partial/\partial z$ is exactly the same as in Cartesian coordinates [3]. For the azimuthal derivative $\partial/\partial\phi$, it is easily obtained by FFT since there is a natural periodicity in the ϕ direction.

Manuscript received January 5, 1999; revised September 11, 2000. This work was supported by the U.S. EPA through a PECASE Grant CR-825-225-010, and by the NSF under CAREER Grant ECS-9702195. This work was done in part while the authors were with New Mexico State University.

The authors are with the Department of Electrical and Computer Engineering, Duke University, Durham, NC 27708 USA (e-mail: qhliu@ee.duke.edu).

Publisher Item Identifier S 0018-926X(01)06378-5.

0018–926X/01$10.00 © 2001 IEEE

The treatment of the ρ derivative is more complicated compared to the Cartesian coordinates, simply because that the boundary at $\rho = 0$ is not an open boundary. One way of treating this is to use Chebyshev pseudospectral method [6] which inevitably increases the number of nodes at $\rho = 0$ and has a stringent stability criterion for Δt. A more efficient way is to form a new function for $0 \leq j_\phi \leq N_\phi/2 - 1$ (assuming N_ϕ is even) such that

$$g(j, j_\phi) = \begin{cases} f(-j-1, j_\phi + N_\phi/2), & \text{for } j = -N_\rho, \ldots, -1 \\ f(j, j_\phi), & \text{for } j = 0, \ldots, N_\rho - 1 \end{cases} \tag{9}$$

where N_ρ and N_ϕ are the number of cells in ρ and ϕ directions, respectively. Then the derivative is found by the FFT of these $N_\phi/2$ new arrays of length $2N_\rho$

$$\frac{\partial g}{\partial \rho} \approx \mathcal{F}_\rho^{-1}\left\{ik_\rho \mathcal{F}_\rho[g]\right\} \tag{10}$$

where $\mathcal{F}_\rho$ and $\mathcal{F}_\rho^{-1}$ denote the forward and inverse FFTs, and k_ρ is the Fourier variable in ρ direction. The PML cells are placed near the outer boundary $\rho = \rho_{\max}$ to eliminate the waves coming from other periods, i.e., to remove the wraparound effect due to the periodicity of the distrete Fourier transform (DFT).

In contrast to Yee's FDTD algorithm, the PSTD algorithm uses a centered grid where all field components are located at the center of each cell. As a result, no field components are actually located at $\rho = 0$. Therefore, the first benefit of this PSTD algorithm is the removal of the singularity at cylindrical axis that is present in the staggered Yee grid.

The second advantage of the cylindrical PSTD algorithm is that it allows a much larger cell than the FDTD method for the same accuracy. For the moderate-size problems shown here (typically $\rho_{\max} \sim 30\lambda$), the saving factor in the grid density (number of cells per wavelength) from the FDTD method is roughly equal to $K = 4$. Thus, for a multidimensional problem, the saving factor in computer memory is K^D, where D is the dimensionality of the problem. Furthermore, K increases with the problem size because for larger problems the required sampling density in the FDTD method increases while that in the PSTD algorithm remains the same. This advantage of the cylindrical PSTD algorithm is the same as that in Cartesian coordinates.

The third and most important advantage of the cylindrical PSTD method is the significantly reduced number of time steps because of the increase cell size $\Delta\rho$. One undesirable property of a cylindrical grid is the high concentration of cells near the axis. Around the axis the cells have an azimuthal length $h = \Delta\rho\Delta\phi/2 = \pi\rho_{\max}/N_\phi N_\rho$. From the stability condition, this requires that the time step $\Delta t \propto h$, that is, $\Delta t \propto 1/N_\rho N_\phi$. Moreover, to satisfy the accuracy at $\rho = \rho_{\max}$, one requires that $N_\phi \propto N_\rho$ to make the dispersion error in the azimuthal direction comparable to other directions. Therefore, for a problem of fixed size (i.e., fixed $\rho_{\max}$), in cylindrical coordinates, in general we have to choose a time step size $\Delta t \propto 1/N_\rho^2$, one order smaller than that required by a Cartesian grid of $\Delta t \propto 1/N_x$. Hence, for large-scale problems, if the PSTD has a cell size ($\Delta\rho$) that is K times that in the FDTD, the FDTD requires roughly K^2 times more time steps than the PSTD algorithm.

Therefore, if the geometry of a problem can be adequately represented by a coarse grid, as is the case in many large-scale problems in geophysical applications, the PSTD method is more efficient than the FDTD method. This is because the spatial derivatives in the PSTD method have a higher order accuracy than the FDTD method. However, note that the time derivative has the same second-order accuracy as in the FDTD method. As a result, for a required accuracy, even though the spatial discretization of the PSTD method can be much coarser, the temporal discretization Δt should be about the same as in the FDTD method for Cartesian coordinates (keeping in mind that the FDTD method requires a much smaller Δt in cylindrical coordinates because of cell clustering, as discussed above). Therefore, if the geometrical modeling requires a fine grid (for example, $\Delta\rho \leq \lambda/10$) to avoid staircasing error, then the FDTD method is more efficient since no FFT is needed and the time step size Δt can be slightly larger [3]. Furthermore, the current PSTD method cannot treat a PEC scatterer because of the Gibbs' phenomenon [3]. Research is underway to address these two issues in the PSTD method.

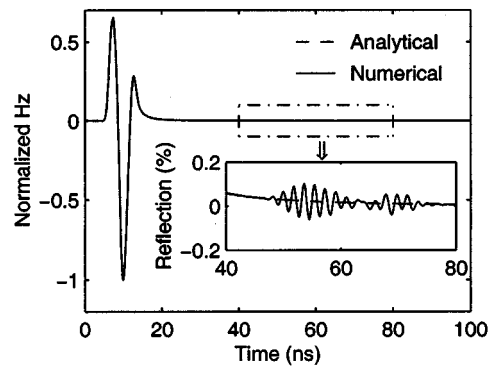

Fig. 1. PSTD and analytical results for a magnetic line source in a 2-D homogeneous medium. The inset magnifies the reflected wave from the PML boundary.

III. Numerical Results

To avoid the Gibbs' phenomenon associated with the delta function in a line (or point) source, here we treat the sources as a spatially smoothed line or point sources [3]. We first model a smoothed magnetic line source in a 2-D free space in polar (ρ, ϕ) coordinates. The source has a Blackman–Harris window time function with center frequency $f_c = 300$ MHz, and is located at $\rho_s = 5.1$ m, $\phi_s = 90°$. The computational domain is meshed by $N_\rho \times N_\phi = 64 \times 128$ cells (including 10 cells of PML near $\rho = \rho_{\max}$) with $\Delta\rho = 0.2$ m, and $\Delta t = 10$ ps. At the frequency $2.5\, f_c$, this discretization is about 2 cells per wavelength. Fig. 1 shows the comparison of the PSTD results and analytical solutions for a receiver at $\rho = 3.1$ m and $\phi = 87.1875°$. The reflection error from the PML is below 0.1%.

For the PSTD code to solve this problem on an HP SPP-2000 Exemplar (1 processor) it takes 890 seconds for the required 10 000 time steps. For an acceptable accuracy, the FDTD method needs $N_\rho \times N_\phi = 256 \times 1024$ cells, requiring 16 times more computer memory. In addition, a much smaller time step $\Delta t \approx 0.36$ ps has to be chosen for stability, requiring 2.75×10^5 time steps for the same problem.

We then simulate a smoothed magnetic point dipole source inside a dielectric sphere of $\epsilon_r = 4$ in a background with $\epsilon_r = 9$. Note that this object is not aligned with the coordinate directions in the vertical (z) direction. The axisymmetric discretization is $N_\rho \times N_z = 64 \times 128$, with $\Delta\rho = \Delta z = 0.044$ m and $\Delta t = 20$ ps. The PSTD results for the ten received waveforms inside and outside the sphere are compared in Fig. 2(b) against the reference FDTD results ($N_\rho \times N_z = 320 \times 640$, $\Delta t = 4$ ps). Excellent agreement is observed from Fig. 2(b) and (c) for the second waveform. This confirms that even at this coarse grid close to the Nyquist sampling rate, the PSTD algorithm produces accurate results for inhomogeneous media. In contrast, the FDTD method takes about 120 times more CPU time to solve this problem.

IV. Conclusion

The cylindrical pseudospectral time-domain method provides efficient time-domain solutions for waves in cylindrical and polar coordinates. As for Cartesian coordinates, the cylindrical PSTD algorithm

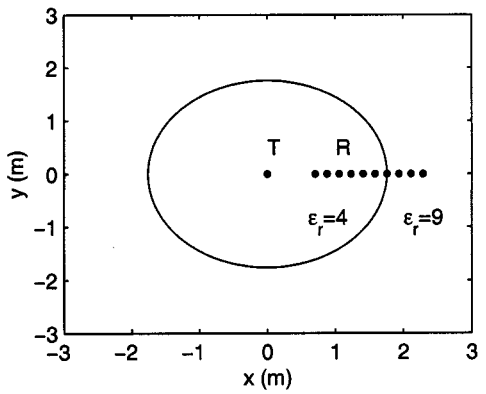

(a)

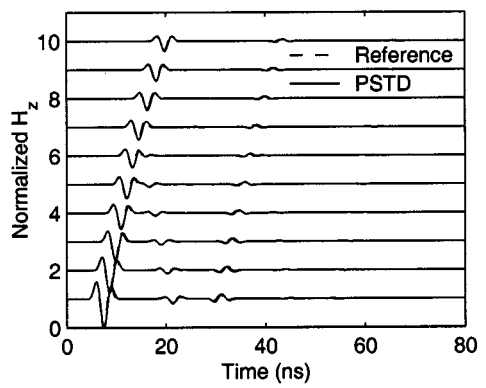

(b)

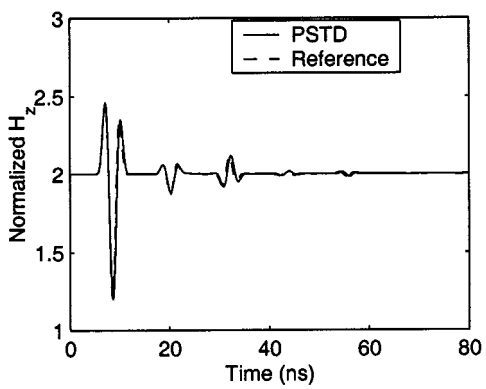

(c)

Fig. 2. PSTD results for a smoothed magnetic point source in a dielectric sphere. (a) Geometry. (b) The array waveforms. (c) The second waveform.

can save substantial amount of computer memory and computation time because of its high accuracy in spatial derivatives achieved by the FFT algorithm. Moreover, the additional advantages of PSTD in cylindrical coordinates include the removal of the singularity at the axis and a substantial reduced number of required time steps compared to the conventional FDTD algorithm.

ACKNOWLEDGMENT

The authors thank two anonymous reviewers for the constructive comments to improve the manuscript.

REFERENCES

[1] K. S. Yee, "Numerical solution of initial boundary value problems involving Maxwell's equations in isotropic media," *IEEE Trans. Antennas Propagat.*, vol. AP-14, pp. 302–307, 1966.

[2] A. Taflove, *Computational Electrodynamics: The Finite Difference Time Domain Method*. Norwood, MA: Artech House, 1995.

[3] Q. H. Liu, "The PSTD algorithm: A time-domain method requiring only two cells per wavelength," *Microwave Opt. Tech. Lett.*, vol. 10, pp. 158–165, 1997.

[4] ——, "The PSTD algorithm for acoustic waves in inhomogeneous, absorptive media," *IEEE Trans. Ultrason., Ferroelect., Freq. Contr.*, vol. 45, no. 4, pp. 1044–1055, 1998.

[5] F. L. Teixeira and W. C. Chew, "PML-FDTD in cylindrical and spherical coordinates," *IEEE Microwave Guided Wave Lett.*, vol. 7, pp. 285–287, 1997.

[6] B. Yang, D. Gottlieb, and J. S. Hesthaven, "Spectral simulations of electromagnetic wave scattering," *J. Comput. Phys.*, vol. 134, pp. 216–230, 1997.

[7] J. He and Q. H. Liu, "A nonuniform cylindrical FDTD algorithm with improved PML and quasi-PML absorbing boundary conditions," *IEEE Trans. Geosci. Remote Sensing*, vol. 37, pp. 1066–1072, 1999.

[8] D. Gottlieb and S. A. Orszag, *Numerical Analysis of Spectral Methods*. Philadelphia, PA: SIAM, 1977.

Statistics of Measured Body Loss for Mobile Phones

Jesper Ø. Nielsen, Gert F. Pedersen, Kim Olesen, and István Z. Kovács

***Abstract*—The variation in body loss for different users of a cellular handset is investigated. Measurements involving 200 test users of mobile communications (GSM) handsets have been performed and statistics are presented for a handset with three types of antennas. Differences in the body loss of up to 10 dB have been observed between users, thus indicating that body loss measurements for handsets should include several test persons. Depending on the antenna type, 8–13 test persons are required to obtain an estimate of the mean body loss with a ± 1 dB confidence interval at a 90% level.**

***Index Terms*—Antenna performance, body loss, handset antennas, mobile communication, radio propagation measurements, user influence.**

I. INTRODUCTION

The overall performance of a cellular system is strongly dependent on the amount of power transmitted and received by the handsets in the system. To a large extent, the multipath propagation channel existing between a base station and a handset determines the amount of received power. However, the power is also depending on the type of receiving antenna, the shape of the handset, etc. In addition, it is well known that the transmitted or received power is reduced due to the presence of the user, where the ratio of power with and without user is denoted the body loss [1]. The body loss may vary significantly depending on the antenna/handset design [2], [3]. Therefore, minimizing the body loss is an obvious way of improving the performance of future handsets. It is important, however, to note that the body loss may vary considerably

Manuscript received February 15, 2000. This work was supported by the TeleDanmark, Denmark.

The authors are with the Center for PersonKommunikation, Aalborg University, Denmark (e-mail: jni@cpk.auc.dk).

Publisher Item Identifier S 0018-926X(01)05637-X.

0018–926X/01$10.00 © 2001 IEEE